Journal of Materials Chemistry C

Accepted Manuscript

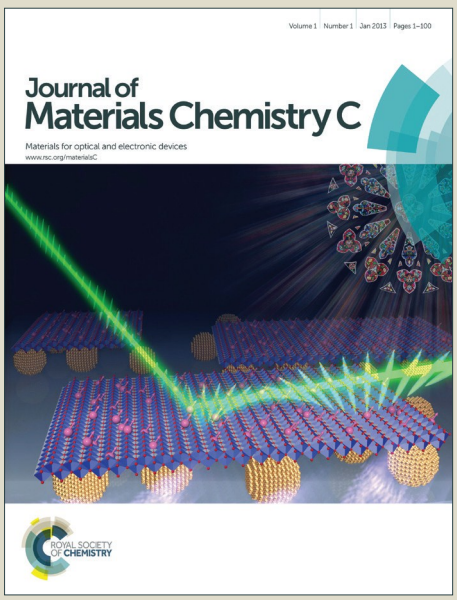

ROYAL SOCIETY OF CHEMISTRY

www.rsc.org/materialsC

Band gap controlling and transformation of monolayer MoS_2-based hetero-bilayers

X.D. Li[1], S.Q. Wu[1,*] and Z.Z. Zhu[1,2,*]
[1]Department of Physics and Institute of Theoretical Physics and Astrophysics, Xiamen University, Xiamen 361005, China
[2]Fujian Provincial Key Laboratory of Theoretical and Computational Chemistry, Xiamen University, Xiamen 361005, China

Abstract

Study of heterostructured bilayer systems is an essential prerequisite for developing two-dimensional nano-electronic devices. Using *ab initio* density functional theory calculations, we investigated the atomic and electronic properties of hetero-bilayers composed of silicene and germanene layers with monolayer MoS_2. Our results show that both Silicene-MoS_2 and Germanene-MoS_2 hetero-bilayers are direct band gap semiconductors. The band gaps of silicene and germanene in hetero-bilayers are opened due to the sublattice symmetry breaking induced by the introduction of the MoS_2 monolayer, indicating that the monolayer MoS_2 makes a good complement to silicene and germanene. Moreover, tunable band gaps in silicene and germanene can be realized by changing the interlayer distance or employing in-plane compressing/stretching. Especially, through compressing or stretching, the Germanene-MoS_2 bilayers realize a transformation from an indirect band gap semiconductor to a direct band gap semiconductor, while the Silicene-MoS_2 bilayers can keep the direct band gaps. Our results in this work provide a new way for designing applications in future MoS_2-based nano devices with controllable band gaps.

Keywords: MoS_2 Monolayer, Silicene, Germanene, Hetero-Bilayer

Introduction

Since the experimental realization of graphene,[1] the two dimensional (2D) materials have attracted tremendous attention from researchers due to their excellent physical and chemical properties.[2-7] Among these graphene-like 2D materials, silicene and germanene (graphene analog of silicon and germanium, respectively) are especially extensively studied from both theoretical and experimental views.[8-13] This is due to the fact that C, Si and Ge atoms all have four electrons in the valence band, which makes the properties of silicene and germanene are very similar to those of graphene.[14-17] Moreover, compared to graphene, silicene and germanene are more preferable in present novel functional electronic devices such as room temperature field effect transistor.[18] Being null gap semiconductors, silicene and germanene fall short of the basic requirement for their possible use in future nanoelectronic and optoelectronic devices. This issue can be solved by introducing a substrate to support silicene or germanene.[8,19-21] However, the single atomic layer grown on metal surface could lead to a significant reduction of its high carrier mobility because of the strong interaction between the 2D material and substrate.[13,22-24] Thus, it is significant to find an ideal substrate for silicene and germanene to not only bring tunable band gaps but also preserve their intrinsic properties.

As is well known, Molybdenum disulfide (MoS_2) is stacked by the S–Mo–S sheets through van der Waals (vdW) interaction.[25] Bulk MoS_2 is an indirect band gap semiconductor, while the 2D MoS_2 monolayer is a direct band gap semiconductor.[2,3,26,27] In addition, the high quality monolayer MoS_2 with the scalable size and excellent electronic properties has been successfully synthesized recently by chemical methods in experiments.[28-33] All these excellent properties make MoS_2 monolayer a potential substrate to support silicene and germanene. Indeed, the electronic and optical properties of heterostructured bilayer systems, which are composed of silicene (or germanene) and other semiconducting

2D materials, have been extensively investigated via first-principles calculations recently.[19,20,34-41] For instance, At room temperature, multiple phases of single crystalline silicene and germanene with different orientations could coexist in silicene/graphene and germanene/graphene bilayer systems.[19] By applying an in-plane homogeneous biaxial strain, the tunable band-gap and quasiparticle effective mass are realizable in graphene/BN bilayer.[34] Optically, optical adsorption of hybrid silicene and graphene nanocomposite is enhanced compared with simplex silicene and graphene.[20] The type-II band offset,[7,35-37] *i.e.*, the conduction band minimum and valence band maximum come from different 2D materials, is also found in hybrid bilayers, which is composed of transition-metal dichalcogenides monolayer and MXene.[38] Hence, the studies of hetero-bilayer systems should be important for further research and possible applications of 2D materials.

In this work, we systematically investigate the atomic and electronic properties of hetero-bilayers composed of silicene and germanene layers with monolayer MoS_2 (labeled as Silicene-MoS_2 and Germanene-MoS_2, respectively) by using density functional theory calculations. Our results show that, unlike the MoS_2 bilayer which is an indirect bandgap semiconductor,[42] the free-standing Silicene-MoS_2 and Germanene-MoS_2 bilayers are both direct band gap semiconductors. The band gaps of silicene and germanene in hetero-bilayers are opened due to the sublattice symmetry breaking induced by the introduction of the MoS_2 monolayer. The two components of heterostructured bilayers could complement each other. On one hand, the band gaps of silicene and germanene in hetero-bilayers are opened due to the introduction of the MoS_2 monolayer. On the other hand, the addition of silicene and germanene significantly increases the electronic conductivity of MoS_2-based heterostructures. In this way, all their different advantages of 2D materials are properly utilized. In addition, a tunable band gap in silicene and germanene can be realized by changing the interlayer distance or employing in-plane compressing/stretching. Our results not only make a

complement explanation to the experimental studies but also suggest a new way to develop the future MoS_2-based nanodevices.

2. Methods

First-principles calculations are performed based on projector-augmented wave (PAW) representations[43] within density functional theory (DFT) as implemented in the Vienna *ab initio* simulation package (VASP).[44,45] Local density approximation (LDA)[46] was employed to describe the exchange–correlation interactions. DFT-LDA provides a good approximation for the band structures characters.[3,25,26] In addition, for layered materials (such as transition metal dichalcogenides and graphite) the lattice constants experimental values exhibit good agreement with the LDA approach.[41] Considering the better consistency between LDA calculations and experimental observations, [3,7,25,26,41] all calculations presented in this work are performed by using the LDA. The plane waves are expanded with energy cut of 420 eV. Brillouin-zone integrations are approximated by using the special ***k***-point sampling of Monkhorst-Pack scheme [47] with a Γ-centered 6×6×3 grid. A supercell with a vacuum of 25 Å in the *z* direction (direction perpendicular to the plane of hetero-bilayer) was set in the present work so that the interaction between two adjacent hetero-bilayers in the periodic arrangement is negligible. The cell parameters and the atomic coordinates of the free hetero-bilayer models are fully relaxed until the force for each atom is lower than 10^{-2} eV/Å (Supplementary Information II). It should be noted that, during the process of changing interlayer distance to control band gaps, the in-plane lattice constants (*a*) were fixed at the equilibrium value of free hetero-bilayers. And for compressed/stretched hetero-bilayers, the lattice parameters were fixed at the compressed/stretched values. The spin-polarized calculations are performed at first, but the results indicate that the hetero-bilayers considered in this work do not exhibit magnetism at their ground states.

3. Results and Discussion

3.1 Atomic Properties

MoS_2, a member of semiconducting layered transition metal dichalcogenides family, is consisted of weakly bonded S-Mo-S single layers (Fig. S1). Within each layer, one Mo atom layer sandwiched between two S layers as shown in Fig. 1 (a). The interaction between Mo-S bonds within each S–Mo–S monolayer is covalent bonding. The symmetry space group of bulk MoS_2 is *P3m1* (point group D_{6h}), while the space group of single layer MoS_2 is *P6m2* with the reduced crystal symmetry D_{3h}.[48,49] Bulk MoS_2 is an indirect band gap semiconductor, while the 2D MoS_2 monolayer is a semiconductor with a direct band gap of 1.9 eV, which is in agreement with the previous theoretical results [2,3,5,26,27] and the experimental value [7] (about 1.8 eV). For the free-standing monolayer MoS_2, the calculated lattice constant is 3.120 Å, which agrees well with the previous values.[2,3,7] In order to set up a proper unit cell for the MoS_2-based hetero-bilayer systems, we first calculate the electronic properties of pristine silicene and germanene. Based on plane wave pseudopotential method, the optimized lattice parameters of silicene and germanene are 3.830 Å and 3.970 Å, respectively. The buckling height (Δ) is the distance between two sublayers in the z-direction, as shown in Fig. 1 (a). Graphene is a one-atom-thick flat sheet,[1] while the most stable isolated silicene and germanene are predicted to have a geometry with low-buckled honeycomb structure for their most stable structures.[8-12] The corresponding buckling of silicene and germanene are Δ = 0.437 Å and 0.647 Å, respectively (Table 1). These structural parameters are in good agreement with previous works.[2,11,50] The buckling heights increase along the row C, Si, Ge. Compared to graphene, silicene and germanene have a preference towards sp^3 hybridization than sp^2 hybridization.[51] The increasing buckling amplitude indicates the transformation from the pure sp^2 bonding to the mixed sp^2–sp^3 bonding. Thus, the sp^3 character also increases

with the increasing buckling height. The lattice constant of silicene (germanene) is 23% (27%) larger than that of monolayer MoS_2. Thus, in order to obtain reasonable results for bilayer systems, low mismatch with a small amount of strain is necessary. Here we imposed a commensurable supercell, in which a 4×4 lateral periodicity of the silicene (or germanene) and 5×5 lateral periodicity of the MoS_2 were employed in the x-y plane (Fig. 1(b)). In this condition, the lattice mismatches for silicene-MoS_2 bilayers and germanene-MoS_2 bilayers are only 1.8%. The present lattice mismatch values are very small by comparison with the previous work.[2,52-54] At first we took the lattice parameter of 5×5 MoS_2 monolayer $\mathbf{5}\boldsymbol{a}_{\boldsymbol{MoS_2}} = \mathbf{15.600}$ Å for the structure optimization, which means the silicene (or germanene) was set to lattice match the MoS_2 monolayer. Then the hetero-bilayers are fully relaxed for both the atomic geometry and the lattice constants. Since the total energies of hetero-bilayer systems are not sensitive to the adsorption site,[52,55] we only studied the bilayer heterostructures with one Si (or Ge) atom on top of the Mo or S atom. The fully optimized geometric structures of hetero-bilayers are shown in Fig. 1(a) and (b).

To evaluate the interlayer interactions between two layers, the binding energy E_b in the hetero-bilayer system is defined as $\boldsymbol{E_b} = -[\boldsymbol{E_{Bilayer}} - (\boldsymbol{E_{Sil/Ger}} + \boldsymbol{E_{MoS_2}})]/\boldsymbol{n_{Mo}}$, where $\boldsymbol{E_{Bilayer}}$, $\boldsymbol{E_{Sil/Ger}}$ and $\boldsymbol{E_{MoS_2}}$ are the total energies in the same supercell for hetero-bilayer, free-standing silicene or germanene sheet and isolated MoS_2 monolayer, respectively. The factor $\boldsymbol{n_{Mo}}$ in the equation corresponds to the number of molybdenum atoms in the supercell, thus, E_b is the interlayer binding energy per MoS_2. The interlayer binding energies per MoS_2 are presented in Table 1. The binding energies between two layers of the hetero-bilayer are 0.127 eV/MoS_2 and 0.141 eV/MoS_2 for the Silicene-MoS_2 and Germanene-MoS_2 bilayers, respectively. The values of binding energy are in the range of physical adsorption, suggesting weak vdW interactions between the atomic layers. The binding energy of Germanene-MoS_2 bilayer is shown to be larger than that of the Silicene-MoS_2 bilayer, suggesting that Germanene-MoS_2

bilayer is more stable than Silicene-MoS_2 bilayer. Germanene structure is more buckled than silicene, which indicates that the interlayer bindings become stronger with an increase in sp^3 hybridization. Within the LDA calculations, the equilibrium separation for the free Silicene-MoS_2 and Germanene-MoS_2 bilayers are 3.056 Å and 3.033 Å, respectively. To examine the optimum spacing between two adjacent atomic layers, we also calculated the binding energies of hetero-bilayer systems with different interlayer distances (Fig. 1(c)). The optimum interlayer distances consistent with the calculated value, which confirms the correctness of our calculation. The interlayer interaction between MoS_2 layer and Silicene (or Germanene) is stronger at shorter interlayer spacing. This again shows that Germanene-MoS_2 bilayer is more stable than Silicene-MoS_2 bilayer. The most stable isolated silicene and germanene are predicted to have a low-buckled honeycomb structure. The amplitudes of the buckling are slightly increased after the introduction of MoS_2 layer and the buckling values in different parts of silicene (or germanene) are different. Furthermore, the buckling increment is influenced by the interlayer distance between MoS_2 sheet and silicone (or germanene), i.e., the buckling amplitude decreases with an increasing interlayer distance (Fig. S3 and Table S1, Supplementary Information III). The buckling values of silicene and germanene in hetero-bilayers increased by 3%~21% (from 0.437 Å to 0.451~0.527 Å) and 5%~15% (from 0.647 Å to 0.678~0.744 Å), respectively. The increase in the value of buckling promotes sp^3 hybridization in Si/Ge atoms of silicone (or germanene) in hetero-bilayer systems. Our results show that both Silicene-MoS_2 and Germanene-MoS_2 bilayers preserve their original hexagonal atomic networks. The calculated lattice parameters of Silicene-MoS_2 and Germanene-MoS_2 hetero-bilayers are 15.530 Å and 15.703 Å, respectively. Compared with the corresponding pristine 2D sheet, the atomic layers in the hetero-bilayers are more or less compressed or expanded. As shown in Table 1, for Silicene-MoS_2 bilayer, the silicene is expanded by 1.4% (from 3.830 Å to 3.883 Å), while the MoS_2

sheet is compressed by 0.4% (from 3.120 Å to 3.106 Å). In the Germanene-MoS_2 bilayer, on the contrary, the germanene sheet is compressed by 1.1% (from 3.970 Å to 3.926 Å), while the MoS_2 sheet is stretched by 0.7% (from 3.120 Å to 3.141 Å). Thus, the Si-Si bond lengths ($d_{Si\text{-}Si}$) of 2.282 Å to 2.294 Å in the bilayer are all larger than that of the isolated silicene, whereas the Ge-Ge bond lengths ($d_{Ge\text{-}Ge}$) of 2.371 Å to 2.380 Å in the bilayer are all shorter than that of the free-standing germanene. As shown in Table 1, the lattice constant of Silicene-MoS_2 is smaller than that of Germanene-MoS_2, while the sheet thickness of Silicene-MoS_2 is bigger than that of Germanene-MoS_2. Therefore, although the Silicene-MoS_2 and Germanene-MoS_2 are two different materials, the atomic bond lengths of Mo-S within the hetero-bilayers are almost the same as that of free-standing MoS_2 monolayer (Supplementary Information IV).

3.2 Band Structures

The band structures of isolated graphene, silicene, germanene and monolayer MoS_2 are depicted in Fig. 2 (a)-(d). Considering the fact that Ge, Si and C have similar electronic configurations, their corresponding 2D materials all have linear dispersion around the Dirac points. The electronic band structures of hetero-bilayers are also presented in Fig. 2 (e)-(f). To help comprehend the band structures of the systems, the contributions of each atomic layer are shown in the same graph. The contributions of silicene, germanene and MoS_2 to the band structures are marked with blue, green and pink dots (where the size of dots are proportional to the contributions), respectively. As shown in Fig. 2(b)-(c), both silicene and germanene are gapless semiconductors with linear dispersions at K point, whereas small band gaps (57.3 meV for Silicene-MoS_2 and 75.5 meV for Germanene-MoS_2) are found in both hetero-bilayer systems. Unlike the superlattices which are metals, the hetero-bilayer systems are semiconductors with direct band gap.[52] In addition, the electronic bands around the Fermi

level mainly came from silicene/germanene layers, indicating that the gaps opened for the superlattices are due to the interactions between silicene/germanene layers only. These gap values are significantly larger than that of graphene-MoS_2 bilayers (2 meV).[55] Since the conventional DFT generally underestimates the energy gap for semiconductors,[56,57] our calculated values just give a lower bound on the real band gaps of hetero-bilayer systems.

3.3 Charge Density Differences

In order to gain further insight into the bonding nature and interlayer interaction of the hetero-bilayer systems, the charge density differences ($\Delta\boldsymbol{\rho}$) of planes parallel to and perpendicular to the atomic layers are shown in Fig. 3. The deformation charge density ($\Delta\boldsymbol{\rho}$) is defined as the difference between the total charge density of the hetero-bilayers and the superposition of independent atomic charge densities placed at the atomic sites of the same hetero-bilayers, *i.e.*, $\Delta\boldsymbol{\rho}(\vec{\boldsymbol{r}}) = \boldsymbol{\rho}(\vec{\boldsymbol{r}}) - \sum_{\mu}\boldsymbol{\rho}_{atom}(\vec{\boldsymbol{r}} - \vec{\boldsymbol{R}}_{\mu})$, where $\vec{\boldsymbol{R}}_{\mu}$ are the atomic positions. The charge density differences of each atomic layers in hetero-bilayers are presented in Fig. 3 (a)-(d). The electron accumulation has been depicted by positive contours (solid orange lines), while the electron depletion represented by negative contours (dashed blue lines). For pristine monolayer MoS_2 (Fig. 3 (e)), it is obviously exhibiting that both Mo and S atoms lose electrons, while there is an electron accumulation of charge density in the bonding region between the Mo and S atoms. This indicates that Mo-S bond is covalent bond. Like Mo-S bond, Si-Si and Ge-Ge bonds in isolated silicene and germanene also behave clear covalent bonding characters (Fig. 3 (f) and (g)). We also find that, within each atomic layer, the atomic bonding of Mo-S, Ge-Ge and Si-Si in both hetero-bilayers are still covalent bonds, indicating that the interactions within each 2D material in hetero-bilayer systems are not affected significantly by the introduction of foreign atomic layers. On the other hand, the charge density differences ($\Delta\boldsymbol{\rho}$) of planes perpendicular to the atomic layers and passing through Mo-

S, Ge-Ge or Si-Si bonds in the hetero-bilayers are shown in Fig. 3 (h)-(i). For the sake of contrast, the charge density differences of the same plane of free-standing silicene, germanene and monolayer MoS_2 are also presented (Fig. 3 (e)-(g)). As presented in Fig. 3 (h)-(i), for inter-layers interactions, except the regions where the Ge/Si atoms are closed to its nearest neighboring S atom, there is no significant charge transfer or charge redistributions in the hetero-bilayers.

3.4 Superlattice versus Hetero-bilayer

We compare all the results with that of the corresponding hybrid superlattices.[52] As for the geometric structures, we find that the value of the buckling of silicene/germanene in hetero-bilayers is less than that in the superlattices.[52] This suggests that the interaction in hetero-bilayers is much weaker than that in superlattice systems. The interlayer distance (d), *i.e.*, the Si-S and Ge-S atomic distances in the Silicene-MoS_2 and Germanene-MoS_2 hetero-bilayers are 3.056 Å and 3.033 Å, respectively. By contrast, the Si-S and Ge-S atomic distances in the Silicene/MoS_2 and Germanene/MoS_2 superlattices are 2.906 Å and 2.891 Å,[52] respectively. This again indicates that the decline of interlayer interactions between two layers in hetero-bilayers as compared to that in the corresponding superlattices. On the other hand, the deformation charge density distribution in the 2D hetero-bilayers and 3D superlattices are very similar to each other. This means that the interaction type between two stacking sheets in the hybrid systems is not influenced by the number of the 2D atomic layers. We also make a comparative study of their band structures. For both hybrid systems, we find that the electronic bands around the Fermi level are mainly contributed by silicene or germanene layers rather than MoS_2 layers. However, unlike the superlattice counterparts which are metals, the hetero-bilayer systems are semiconductors with direct band gaps. This result shows that the direct bandgap monolayer MoS_2 is a good complement to the null gap

silicene and germanene, which makes monolayer MoS_2 an ideal substrate for silicene and germanene. It is important to point out that although the gaps are also opened in superlattices, the small gap openings of silicene and germanene are not at the Fermi level. Thus, the small gaps of superlattices may have no important significance for real applications, and the importance should be only in the theoretical respect. However, for Silicene-MoS_2 and Germanene-MoS_2 hetero-bilayers, the Fermi level lies between the valence band maximum and the conduction band minimum, which makes MoS_2-based hetero-bilayers promising candidates for future nanodevices.

3.5 Band Gap Controlling

As mentioned above, to minimize the lattice mismatch between the stacking sheets, for heterostructured bilayer systems, we employed a supercells consisting of and 5×5 unit cells of MoS_2 monolayer and 4×4 unit cells of silicene (and germanene). Although the lattice mismatch values are very small, both layers still have to be compressed or stretched to match each other. Thus, it is significant to investigate the electronic properties of compressed or stretched hetero-bilayers. We carried out studies on the electronic band structures of compressed (with −1.5% decreases in lattice parameters) and stretched (with +1.5% increases in lattice parameters) hetero-bilayers, which are given in Fig. 4 and Table 2. The band structures of unstrained Silicene-MoS_2 and Germanene-MoS_2 hetero-bilayers are also depicted in the middle of Fig. 4 for comparisons. It can be seen that both magnitude and type of band gaps can be varied by compressing or stretching the lattice constants. In both bilayer systems, at the K point, the value of band gaps decrease monotonically with increase in lattice parameters. The size of strain-induced band gap of Silicene-MoS_2 and Germanene-MoS_2 hetero-bilayers are in the range of 49.5~68.0 meV and 67.2~84.6 meV, respectively. For Silicene-MoS_2 hetero-bilayers, the compressed or stretched systems are still

semiconductors with direct band gaps at the K point in BZ. However, this result is not valid for Germanene-MoS_2 hetero-bilayers. In the case of Germanene-MoS_2 bilayer system, as the lattice constant is increased, the bands (at Γ point) move towards the deeper energy level. Hence, through compressing or stretching, the hetero-bilayers realize the transformation of semiconductor from an indirect band gap to a direct one.

Except for compressing and stretching methods, the band gaps of heterostructures can also be affected by the interlayer distance between two adjacent layers.[55,58] Therefore, we calculate the band gap values of the hybrid bilayer system with various interlayer spacing. It can be seen from Table 3, when the interlayer distance is shorter than the equilibrium value (3.06 Å for Silicene-MoS_2 hetero-bilayer and 3.03 Å for Germanene-MoS_2 hetero-bilayer), the band gap increases with the increasing interlayer distance. Then the gaps reached its maximum value at the equilibrium state. After that, the band gap decreases with the increasing interlayer spacing, due to an increased interaction between the adjacent layers. The magnitude of tunable band gap of Silicene-MoS_2 and Germanene-MoS_2 hetero-bilayers are in the range of 1.4~57.3 meV and 10.5~75.5 meV, respectively. In the process of changing the interlayer distance, both hetero-bilayers maintain their direct band gap semiconductor properties. These results offer a convenient way to control the band gaps of heterostructured bilayers.

4. Conclusion

In conclusion, by employing *ab initio* calculations, we investigated the structural and electronic properties of Silicene-MoS_2 and Germanene-MoS_2 bilayer heterostructures. The band gaps of silicene and germanene are both opened at the *K*-point due to the sublattice symmetry broken caused by the introduction of monolayer MoS_2. Thus, the silicene (or germanene) adsorbed on the MoS_2 monolayer is no longer metal but semiconductor with

finite direct band gap. Moreover, the values of band gap could be controlled by changing the interlayer distance or by in-plane compressing/stretching. The band gap size of Silicene-MoS_2 and Germanene-MoS_2 hetero-bilayers are in the range of 1.4~68.0 meV and 10.5~84.6 meV, respectively. The tunable band structures make Silicene-MoS_2 and Germanene-MoS_2 hetero-bilayers promising candidates for future MoS_2-based nanodevices.

Acknowledgments

This work is supported by the National 973 Program of China (Grant No. 2011CB935903), the Fundamental Research Funds for the Central Universities (Grant No. 20720150033), the National Natural Science Foundation of China (Grant Nos. 11104229, 11004165, 21233004), and the Natural Science Foundation of Fujian Province of China (Grant No. 2015J01030).

Reference

1. Novoselov, K. S.; Geim, A. K.; Morozov, S. V.; Jiang, D.; Zhang, Y.; Dubonos, S. V.; Grigorieva, I. V.; Firsov, A. A. Electric Field Effect in Atomically Thin Carbon Films. *Science*, **2004**, *306*, 666-669.
2. Lebègue, S.; Eriksson, O. Electronic structure of two-dimensional crystals from ab initio theory. *Phys. Rev. B*, **2009**, *79*, 115409.
3. Ding, Y.; Wang, Y.; Ni, J.; Shi, L.; Shi, S.; Tang, W. First principles study of structural, vibrational and electronic properties of graphene-like MX_2 (M=Mo, Nb,W,Ta;X=S, Se,Te) monolayers. *Physica B*, **2011**, *406*, 2254-2260.
4. Castro Neto, A. H.; Guinea, F.; Peres, N. M. R.; Novoselov, K. S.; Geim, A. K. The electronic properties of graphene. *Rev. Mod. Phys.*, **2009**, *81*, 109-162.
5. Ma, Y.; Dai, Y.; Guo, M.; Niu, C.; Lu, J.; Huang, B. Electronic and magnetic properties of perfect, vacancy-doped, and nonmetal adsorbed MoSe2, $MoTe_2$ and WS_2 monolayers. *Phys. Chem. Chem. Phys.*, **2011**, *13*, 15546-15553.
6. Ma, Y.; Dai, Y.; Guo, M.; Niu, C.; Lu, J.; Huang, B. Strain-induced magnetic transitions in half-

fluorinated single layers of BN, GaN and graphene. *Nanoscale*, **2011**, *3*, 2301-2306.

7. Mak, K. F.; Lee, C.; Hone, J.; Shan, J.; Heinz, T. F. Atomically Thin MoS_2: A New Direct-Gap Semiconductor. *Phys. Rev. Lett.*, **2010**, *105*, 136805.
8. Guo, Z. X.; Furuya, S.; Iwata, J.; Oshiyama, A. Absence and presence of Dirac electrons in silicene on substrates. *Phys. Rev. B*, **2013**, *87*, 235435.
9. O'Hare, A.; Kusmartsev, F. V.; Kugel, K. I. A Stable "Flat" Form of Two-Dimensional Crystals: Could Graphene, Silicene, Germanene Be Minigap Semiconductors? *Nano Lett.*, **2012**, *12*, 1045-1052.
10. Quhe, R.; Fei, R.; Liu, Q.; Zheng, J.; Li, H.; Xu, C.; Ni, Z.; Wang, Y.; Yu, D.; Gao, Z.; Lu, J. Tunable and sizable band gap in silicene by surface adsorption. *Sci. Rep.*, **2012**, *2*, 853.
11. Ni, Z.; Liu, Q.; Tang, K.; Zheng, J.; Zhou, J.; Qin, R.; Gao, Z.; Yu, D.; Lu, J. Tunable Bandgap in Silicene and Germanene. *Nano Lett.*, **2012**, *12*, 113-118.
12. Ye, M.; Quhe, R.; Zheng, J.; Ni, Z.; Wang, Y.; Yuan, Y.; Tse, G.; Shi, J.; Gao, Z.; Lu, J. Tunable band gap in germanene by surface adsorption. *Physica E*, **2014**, *59*, 60-65.
13. Lalmi, B.; Oughaddou, H.; Enriquez, H.; Kara, A.; Vizzini, S.; Ealet, B.; Aufray, B. Epitaxial growth of a silicene sheet. *Appl. Phys. Lett.*, **2010**, *97*, 223109.
14. Cahangirov, S.; Topsakal, M.; Aktürk, E.; Şahin, H.; Ciraci, S. Two- and One-Dimensional Honeycomb Structures of Silicon and Germanium. *Phys. Rev. Lett.*, **2009**, *102*, 236804.
15. Şahin, H.; Cahangirov, S.; Topsakal, M.; Bekaroglu, E.; Akturk, E.; Senger, R. T.; Ciraci, S. Monolayer honeycomb structures of group-IV elements and III-V binary compounds: First-principles calculations. *Phys. Rev. B*, **2009**, *80*, 155453.
16. Liu, C.; Feng, W.; Yao, Y. Quantum Spin Hall Effect in Silicene and Two-Dimensional Germanium. *Phys. Rev. Lett.*, **2011**, *107*, 076802.
17. Houssa, M.; Scalise, E.; Sankaran, K.; Pourtois, G.; Afanas'ev, V. V.; Stesmans, A. Electronic properties of hydrogenated silicene and germanene. *Appl. Phys. Lett.*, **2011**, *98*, 223107.
18. Vogt, P.; Padova, P. D.; Quaresima, C.; Avila, J.; Frantzeskakis, E.; Asensio, M. C.; Resta, A.; Ealet, B.; Lay, G. L. Silicene: Compelling Experimental Evidence for Graphenelike Two-Dimensional Silicon. *Phys. Rev. Lett.*, **2012**, *108*, 155501.
19. Cai, Y.; Chuu, C.; Wei, C. M.; Chou, M. Y. Stability and electronic properties of two-dimensional silicene and germanene on graphene. *Phys. Rev. B.*, **2013**, *88*, 245408.

20. Hu W.;, Li, Z.; Yang, J. Structural, electronic, and optical properties of hybrid silicene and graphene Nanocomposite. *J. Chem. Phys.*, **2013**, 139, 154704.

21. Kaloni, T. P.; Gangopadhyay, S.; Singh, N.; Jones, B.; Schwingenschlögl, U. Electronic properties of Mn-decorated silicene on hexagonal boron nitride. *Phys. Rev. B*, **2013**, *88*, 235418.

22. Feng, B.; Ding, Z.; Meng, S.; Yao, Y.; He, X.; Cheng, P.; Chen, L.; Wu, K. Evidence of Silicene in Honeycomb Structures of Silicon on Ag(111). *Nano Lett.*, **2012**, *12*, 3507-3511.

23. Enriquez, H.; Vizzini, S.; Kara, A.; Lalmi, B.; Oughaddou, H. Silicene structures on silver surfaces. *J. Phys.: Condens. Matter*, **2012**, *24*, 314211.

24. Fleurence, A.; Friedlein, R.; Ozaki, T.; Kawai, H.; Wang, Y.; Yamada-Takamura, Y. Experimental Evidence for Epitaxial Silicene on Diboride Thin Films. *Phys. Rev. Lett.*, **2012**, *108*, 245501.

25. Kuc, A.; Zibouche, N.; Heine, T. Influence of quantum confinement on the electronic structure of the transition metal sulfide TS_2. *Phys. Rev. B*, **2011**, *83*, 245213.

26. Splendiani, A.; Sun, L.; Zhang, Y.; Li, T.; Kim, J.; Chim, C.; Galli, G.; Wang, F. Emerging Photoluminescence in Monolayer MoS_2. *Nano Lett.*, **2010**, *10*, 1271-1275.

27. Kadantsev, E. S.; Hawrylak, P. Electronic structure of a single MoS_2 monolayer. *Solid State Commun.*, **2012**, *152*, 909-913.

28. Altavilla, C.; Sarno, M.; Ciambelli, P. A Novel Wet Chemistry Approach for the Synthesis of Hybrid 2D Free-Floating Single or Multilayer Nanosheets of MS2@oleylamine (M=Mo, W). *Chem. Mater.* **2011**, *23*, 3879-3885.

29. Coleman, J. N.; Lotya, M.; O'Neill, A.; Bergin, S. D.; King, P. J.; Khan, U.; Young, K.; Gaucher, A.; De, S.; Smith, R. J.; Shvets, I. V.; Arora, S. K.; Stanton, G.; Kim, H. Y.; Lee, K.; Kim, G. T.; Duesberg, G. S.; Hallam, T.; Boland, J. J.; Wang, J. J.; Donegan, J. F.; Grunlan, J. C.; Moriarty, G.; Shmeliov, A.; Nicholls, R. J.; Perkins, J. M.; Grieveson, E. M.; Theuwissen, K.; McComb, D. W.; Nellist, P. D.; Nicolosi, V. Two-Dimensional Nanosheets Produced by Liquid Exfoliation of Layered Materials. *Science*, **2011**, *331*, 568-571.

30. Park, W.; Baik, J.; Kim, T. Y.; Cho, K.; Hong, W. K.; Shin, H. J.; Lee, T. Photoelectron Spectroscopic Imaging and Device Applications of Large-Area Patternable Single-Layer MoS_2 Synthesized by Chemical Vapor Deposition. *ACS Nano*, **2014**, *8*, 4961-4968.

31. Yin, W. Y.; Yan, L.; Yu, J.; Tian, G.; Zhou, L. J.; Zheng, X. P.; Zhang, X.; Yong, Y.; Li, J.; Gu, Z. J.;

Zhao, Y. L. High-Throughput Synthesis of Single-Layer MoS2 Nanosheets as a Near-Infrared Photothermal-Triggered Drug Delivery for Effective Cancer Therapy. *ACS Nano*, **2014**, *8*, 6922-6933.

32. Yu, Y. F.; Li, C.; Liu, Y.; Su, L. Q.; Zhang, Y.; Cao, L. Y. Controlled Scalable Synthesis of Uniform, High-Quality Monolayer and Few-layer MoS_2 Films. *Sci. Rep.*, **2013**, *3*, 1866.

33. Varrla, E.; Backes, C.; Paton, K. R.; Harvey, A.; Gholamvand, Z.; McCauley, J.; Coleman, J. N. Large-Scale Production of Size-Controlled MoS_2 Nanosheets by Shear Exfoliation. *Chem. Mater.*, **2015**, *27*, 1129-1139.

34. Behera, H.; Mukhopadhyay, G. Strain-tunable band gap in graphene/h-BN hetero-bilayer. *J. Phys. Chem. Sol.*, **2012**, *73*, 818-821.

35. Tongay, S.; Zhou, J.; Ataca, C.; Lo, K.; Matthews, T. S.; Li, J.; Grossman. J. C.; Wu, J. Thermally Driven Crossover from Indirect toward Direct Bandgap in 2D Semiconductors: $MoSe_2$ versus MoS_2. *Nano Lett.*, **2012**, *12*, 5576-5580.

36. Radisavljevic, B.; Radenovic, A.; Brivio, J.; Giacometti, V.; Kis, A. Single-layer MoS_2 transistors. *Nature Nanotech.*, **2011**, *6* 147-150.

37. Sahin, H.; Tongay, S.; Horzum, S.; Fan, W.; Zhou, J.; Li, J.; Wu, J.; Peeters, F. M. Anomalous Raman spectra and thickness-dependent electronic properties of WSe_2. *Phys. Rev. B*, **2013**, *87*, 165409.

38. Ma, Z.; Hu, Z.; Zhao, X.; Tang, Q.; Wu, D.; Zhou, Z.; Zhang, L. Tunable Band Structures of Heterostructured Bilayers with Transition-Metal Dichalcogenide and MXene Monolayer. *J. Phys. Chem. C*, **2014**, *118*, 5593-5599.

39. Wang, Z. L.; Chen, Q.; Wang, J. L. Electronic Structure of Twisted Bilayers of Graphene/MoS_2 and MoS_2/MoS_2. *J. Phys. Chem. C*, **2015**, *119*, 4752-4758.

40. Sharma, M.; Kumar, A.; Ahluwalia, P. K.; Pandey, R. Strain and electric field induced electronic properties of two-dimensional hybrid bilayers of transition-metal dichalcogenides. *J. Appl. Phys.*, **2014**, *116*, 063711.

41. Terrones, H.; López-Urías, F.; Terrones, M. Novel hetero-layered materials with tunable direct band gaps by sandwiching different metal disulfides and diselenides. *Sci. Rep.*, **2013**, *3*, 1549.

42. Liu, Q.; Li, L.; Li, Y.; Gao, Z.; Chen, Z.; Lu, J. Tuning Electronic Structure of Bilayer MoS_2 by Vertical Electric Field: A First-Principles Investigation. *J. Phys. Chem. C*, **2012**, *116*, 21556−21562.

43. Kresse, G.; Joubert, D. From ultrasoft pseudopotentials to the projector augmented-wave method. *Phys.*

Rev. B, **1999**, *59*, 1758-1775.

44. Kresse, G.; Furthmüller, J. Efficiency of ab-initio total energy calculations for metals and semiconductors using a plane-wave basis set. *Comput. Mater. Sci.*, **1996**, *6*, 15-50.

45. Kresse, G.; Furthmüller, J. Efficient iterative schemes for ab initio total-energy calculations using a plane-wave basis set. *Phys. Rev. B*, **1996**, *54*, 11169-11186.

46. Ceperley, D. M.; Alder, B. J. Ground State of the Electron Gas by a Stochastic Method. *Phys. Rev. Lett.*, **1980**, *45*, 566-569.

47. Monkhorst, H. J.; Pack, J. Special points for Brillouin-zone integrations. *Phys. Rev. B*, **1976**, *13*, 5188-5192.

48. Xiao, D.; Liu, G. B.; Feng, W.; Xu, X.; Yao, W. Coupled Spin and Valley Physics in Monolayers of MoS2 and Other Group-VI Dichalcogenides. *Phys. Rev. Lett.*, **2012**, *108*, 196802.

49. Molina-Sánchez, A.; Wirtz, L. Phonons in single-layer and few-layer MoS_2 andWS_2. *Phys. Rev. B*, **2011**, *84*, 155413.

50. Garcia, J. C.; de Lima, D. B.; Assali, L. V. C.; Justo, J. F. Group IV Graphene- and Graphane-Like Nanosheets. *J. Phys. Chem. C*, **2011**, *115*, 13242-13246.

51. Matthes, L.; Olivia Pulci, O.; Bechstedt, F. Massive Dirac quasiparticles in the optical absorbance of graphene, silicene, germanene, and tinene. *J. Phys.: Condens. Matter*, **2013**, *25*, 395305.

52. Li, X. D.; Wu, S. Q.; Zhou, S.; Zhu, Z. Z. Structural and electronic properties of germanene/MoS_2 monolayer and silicene/MoS_2 monolayer Superlattices. *Nanoscale Res. Lett.*, **2014**, *9*, 110.

53. Li, W.; Chen, J.; He, Q.; Wang, T. Electronic and elastic properties of MoS_2. *Physica B*, **2010**, *405*, 2498-2502.

54. Seifert, G.; Terrones, H.; Terrones, M.; Jungnickel, G.; Frauenheim, T. Structure and Electronic Properties of MoS_2 Nanotubes. *Phys. Rev. Lett.*, **2000**, *85*, 146-149.

55. Ma, Y.; Dai, Y.; Guo, M.; Niu, C.; Huang, B. Graphene adhesion on MoS_2 monolayer: An ab initio study. *Nanoscale*, **2011**, *3*, 3883-3887.

56. Perdew, J. P.; Levy, M. Physical Content of the Exact Kohn-Sham Orbital Energies: Band Gaps and Derivative Discontinuities. *Phys. Rev. Lett.*, **1983**, *51*, 1884-1887.

57. Sham, L. J.; Schluter, M. Density-Functional Theory of the Energy Gay. *Phys. Rev. Lett.*, **1983**, *51*, 1888-1891.

58. Giovannetti, G.; Khomyakov, P. A.; Brocks, G.; Kelly, P. J.; Brink, J. V. D. Substrate-induced band gap in graphene on hexagonal boron nitride: Ab initio density functional calculations. *Phys. Rev. B*, **2007**, *76*, 073103.

Table

Table 1. Binding energy (E_b), lattice constants (a,b), averaged interlayer distance (d), buckling (Δ), bond lengths (d_{Si-Si}, d_{Ge-Ge}, d_{Mo-S}) and MoS_2 sheet thickness (h_{s-s}) of hetero-bilayer systems.

System	E_b(per MoS_2) (eV)	a=b (Å)	d (Å)	Δ_{Si} (Å)	Δ_{Ge} (Å)	d_{Si-Si} (Å)	d_{Ge-Ge} (Å)	d_{Mo-S} (Å)	h_{s-s} (Å)
Silicene-MoS_2	0.127	15.530	3.056	0.451~0.527	/	2.282~2.294	/	2.373~2.394	3.126~3.139
Germanene-MoS_2	0.141	15.703	3.033	/	0.678~0.744	/	2.371~2.380	2.380~2.400	3.110~3.115
Silicene	/	15.320	/	0.437	/	2.251	/	/	/
Germanene	/	15.880	/	/	0.647	/	2.381	/	/
Monolayer MoS_2	/	15.600	/	/	/	/	/	2.382	3.114

Table 2. Lattice parameters and band gap at K-point for compressed/stretched hetero-bilayers.

hetero-bilayer	a=b (Å)			Band gap at K-point (meV)		
	Compressed (-1.5%)	Unstrained	Stretched (+1.5%)	Compressed (-1.5%)	Unstrained	Stretched (+1.5%)
Silicene-MoS_2	15.297	15.530	15.763	68.0	57.3	49.5
Germanene-MoS_2	15.467	15.703	15.938	84.6	75.5	67.2

Table 3. Band gaps for hetero-bilayer systems with different interlayer spacing.

Interlayer spacing (Å)	Band gap (meV)	
	Silicene-MoS_2	Germanene-MoS_2
2.5	1.4	10.5
2.75	30.6	49.5
3.06[a]/3.03[b]	57.3	75.5
3.25	42.3	57.9
3.5	33.6	45.5

[a]equilibrium interlayer distance for Silicene-MoS_2 hetero-bilayer;

[b]equilibrium interlayer distance for Germanene-MoS_2 hetero-bilayer.

Figure

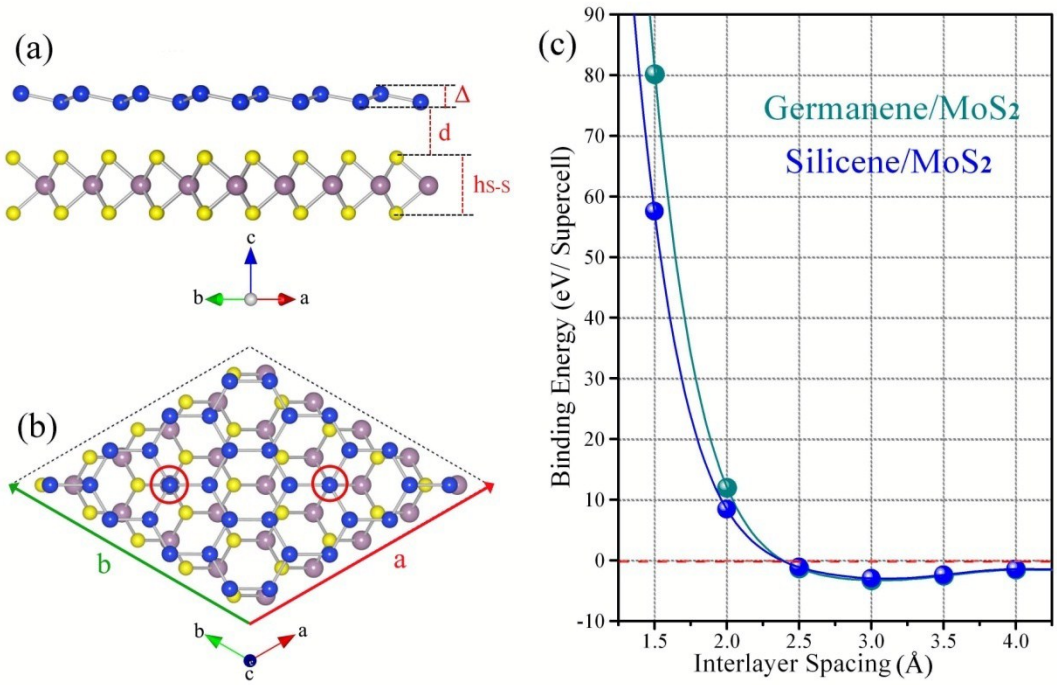

Fig 1. (Color online). (a) Side and (b) top views of hetero-bilayer systems. (c) Binding energies of hetero-bilayer systems as a function of the interlayer spacing between the Sulfur layer of monolayer MoS_2 and its nearest Germanium (green) and Silicon (blue) layers.

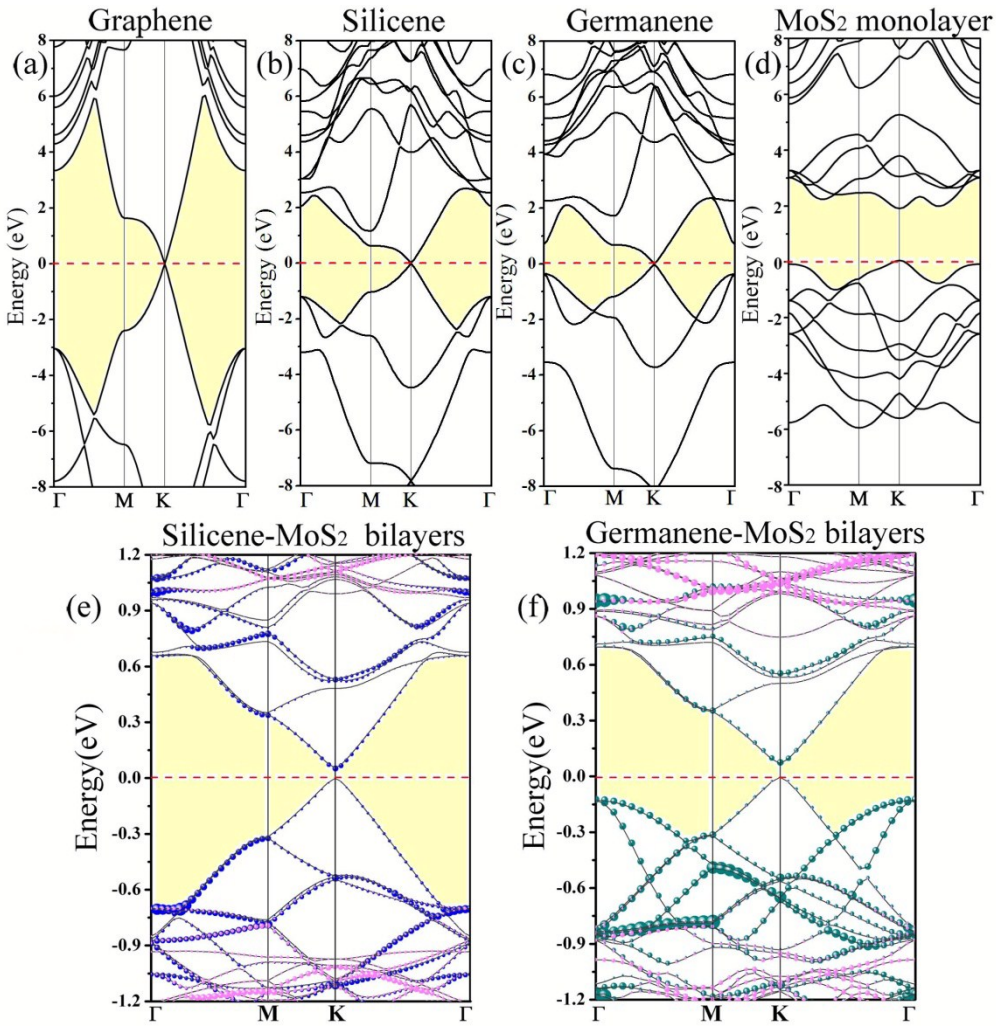

Fig 2. (Color online). Band structures of (a) graphene, (b) low-buckled silicene, (c) low-buckled germanene, (d) MoS_2 monolayer, (e) Silicene-MoS_2 hetero-bilayer and (f) Germanene-MoS_2 hetero-bilayer. Contribution from silicene, germanene and MoS_2 layers to the band structures of the bilayers are shown with blue, green and pink circle dots, respectively. Red dashed lines represent the Fermi level.

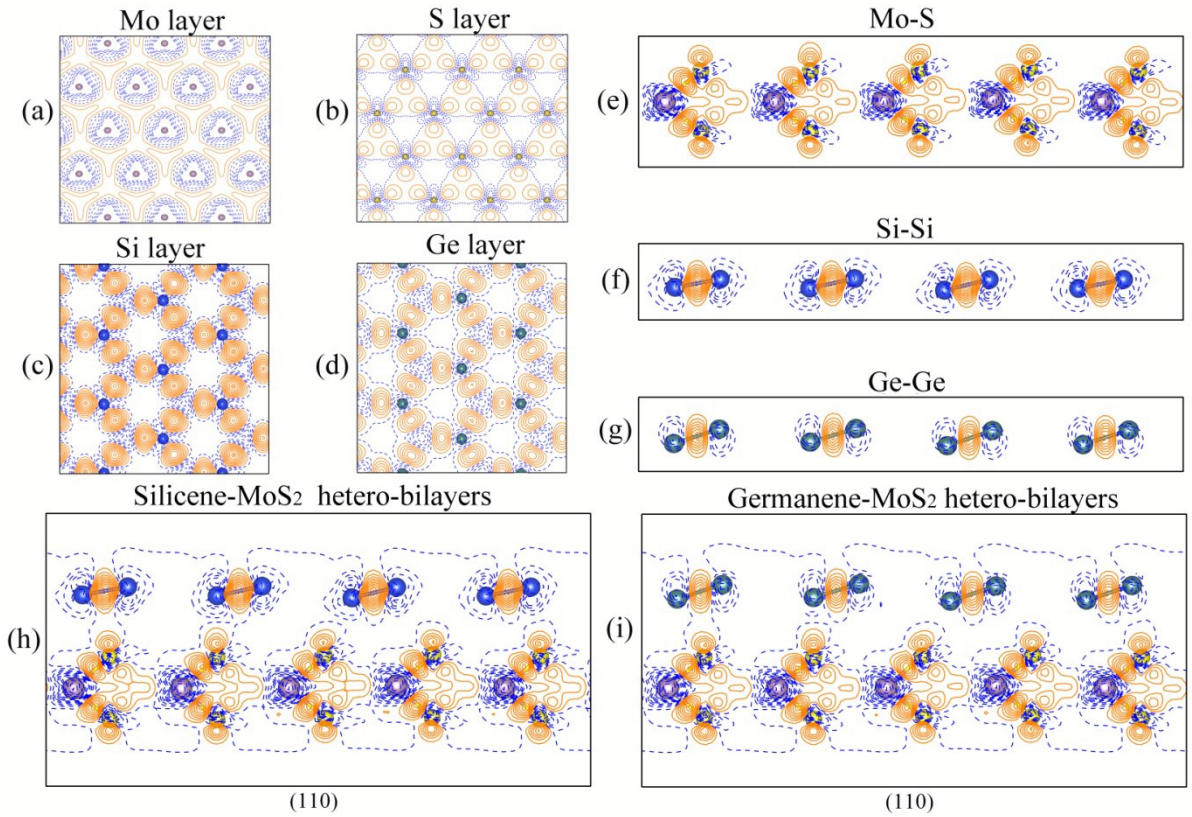

Fig 3. (Color online). Deformation charge density (Δρ) for hetero-bilayer systems. Δρ of planes passing through (a) Mo-, (b) S- (c) Si- and (d) Ge-layers in the bilayers. (e)-(g) Δρ of planes perpendicular to the atomic layers and passing through Mo-S, Si-Si and Ge-Ge bonds in the pristine 2D materials. (h) and (i) are Δρ of planes perpendicular to the atomic layers and passing through Mo-S, Ge-Ge or Si-Si bonds in the hetero-bilayers. Orange and blue lines correspond to $\Delta\rho > 0$ and $\Delta\rho < 0$, respectively.

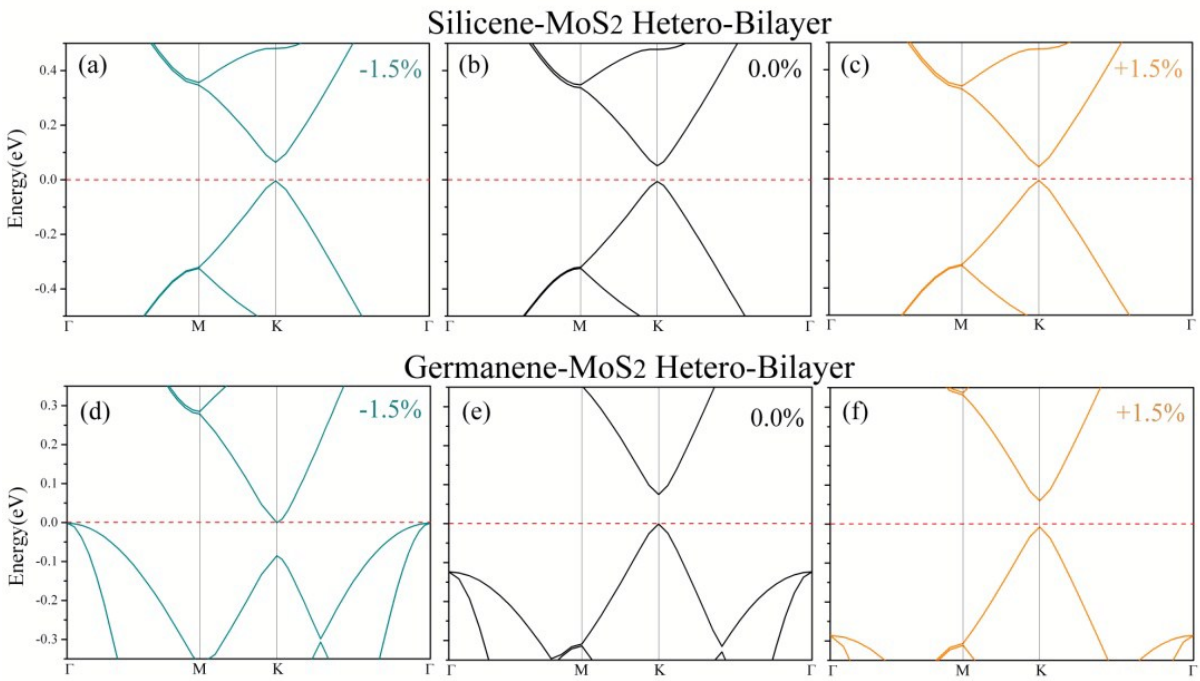

Fig 4. (Color online). Electronic band structures of the (a) and (d) compressed, (b) and (e) free, and (c) and (f) stretched hetero-bilayer systems.

Tunable band gaps of MoS_2-based hetero-bilayers can be realized by changing the interlayer spacing or employing in-plane compressing/stretching.